Hybrid Nanofluid Slip Flow over a Permeable Sheet with Radiative Heat flux, Variable Thermal Conductivity and Heat Source.

Abstract

Purpose – This aims to investigate heat and mass transfer characteristics of hybrid Nano fluid slip flow over a permeable sheet with radiative heat flux, variable thermal conductivity and heat source.

Formulation/methodology/approach – Formulated Mathematical equations are transformed into self-similar equations using similarity transformation. Boundary value problem solver in MATLAB was used to solve the system of reduced similarity equations. In this study thorough examination was made on flow and heat transfer properties for various values of variable thermal conductivity parameter, thermal radiation and heat source. Validation of the present results with published results are in excellent agreement.

Findings – it is noticed that increase in radiative parameter attracts increase in temperature of the fluid at the shrinking region. It indicates that on shrinking region heat absorption take place with increase in value of variable thermal conductivity parameter (Ɛ). The velocity of the fluid is appreciated with increase in silver volume fraction (ϕ_2) and depreciates with increase in velocity slip parameter (P). Increase in velocity slip parameter decreases the local skin friction (P) and local Nusselt number is appreciated by increasing radiation parameter (R).Heat absorption is noticed with increase in variable thermal conductivity, silver volume fraction (ϕ_2) and heat source/sink parameter (Q).

Practical implication – In practice the investigation of effects of hybrid nanofluid flow over a permeable sheet with radiative heat flux, variable thermal conductivity and heat source have real-life and industrial applications, for example manufacturing, cooling electrical devices, biomedical, military etc.

Key words: Variable Thermal Conductivity, Radiative Heat flux, Heat Source and Slip condition.

Nomenclature

u, v	Velocity in x and y directions respectively.
u_w	Surface velocity.
v_w	Wall mass transfer velocity.
L	Characteristics length
T	Fluid temperature
T_w	Temperature of the fluid at the wall
T_∞	Temperature of the fluid away from the wall
γ	Heat generation parameter
λ	Stretching/shrinking parameter

P_1 Velocity slip factor

Q_1 Thermal slip factor

ρ_f Fluid density

ρ_{hnf} Hybrid nanofluid density

$\left(\rho C_p\right)_f$ Fluid heat capacity

$\left(\rho C_p\right)_{hnf}$ Hybrid nanofluid heat capacity

μ_f Fluid dynamics viscosity

μ_{hnf} Hybrid nanofluid dynamics viscosity

k_f Fluid thermal conductivity

k_{hnf} Hybrid nanofluid thermal conductivity

f Dimensionless velocity

θ Dimensionless temperature

Pr Prandlt number

q Heat generation rate constant

P Dimensionless velocity slip parameter

Q Dimensionless thermal slip parameter

$\phi_{s1,}\phi_{s2}$ Nanoparticles volume fraction for aluminium and silver respectively

ε Variable thermal conductivity parameter

S Wall mass transfer parameter

C_f Local skin friction coefficient

Nu_x Local Nusselt number

Re_x Local Renold's number

t Time

τ Dimensionless time variable

Ω Eigenvalue

Introduction

Effects of thermal conductivity in the studies of heat and mass transfer attracted attention of many researchers around the globe. Increase in its expansion and applicability has resulted to the advent of nano-fluid which play important role in thermal conductivity and resulted in in-depth analysis on thermal management of electronic devices. Its application in the area of cooling engines as coolant and electronics does not come with surprise since metallic substances (nano particles) conduct heat more than ordinary liquid (base fluid).

Relevant literature on nanofluid and hybrid nanofluid were reviewed. Nanofluid flow has become area of interest for many researchers globally. Researches conducted were either experimental or theoretical studies and in most cases the two results found to be in agreement. Measurement of local heat transfer coefficient along the tube in laminar flow of nanofluids, was conduscted by Wen and Ding, [1]. It was discovered that the increase in heat transfer coefficient is greatest at the entry length region and enhancement increases with particles concentration. Roy *et al.* [2], studied heat transfer and fluid flow of nanofluids in laminar radial flow cooling system. In their research established the importance of nanofluid as interesting alternative to conventional coolants. Devi and Andrews [3] investigated laminar boundary flow of nanofluid over a flat plate. Analytical solution of natural convection flow of a nanofluid over a linearly stretching sheet in the presence of magnetic field, was presented by Hamad, [4]. Maripala and Kishan [5], studied MHD nanofluid radiating stretching sheet with chemical reaction and heat source/sink. It was observed that when the strength of the magnetic field increase the velocity gradient at the interface has been diminishes, the temperature profiles increases with the increase in magnetic field parameter. Aly and Pop [5], studied MHD flow and heat transfer over a permeable Stretching /shrinking sheet in a hybrid nanofluid with a convective boundary condition It was concluded that the hybrid nanofluid causes more reduction in temperature profile unlike the mono nanofluid when the magnetic field, suction and copper volume fraction parameters are amplified. Dual solution and stability analysis of a hybrid nanofluid over a stretching/shrinking sheet executing MHD flow, was investigated by Lund *et al*., [7]. Zainal *et al*., [8] investigated stability analysis of MHD hybrid nanofluid flow over a stretching/shrinking sheet with quadratic velocity. Xuan and Roezil [9], examined the Conceptions for heat transfer correlation of nanofluids and found out that thermal dispersion which takes place due to random movement of particles takes a major role in increasing heat transfer rate between the fluid and the wall. Huang and Yih [10] presented Non-linear radiation and variable viscosity effects on free convection of a power-law nanofluid over a truncated cone in porous medium with zero nanoparticles flux and internal heat generation. Wahid et al. [11] demonstrated hybrid nanofluid slip flow over an exponentially stretching/shrinking permeable sheet with heat generation. It was observed that an increase in the values of porosity and heat generation parameter resulted in increase in the thermal conductivity of the nanofluid. Thermal energy transport of radioactive nanofluid flow submerged with microorganism with zero mass flux condition was analysed by Gangadha *et al.* [12]. Iyahraja et al., [13] analysed on investigation on silver-water nanofluid for development of new viscosity correlation. Rajesh and Sheremet [14] presented natural convection on ternary hybrid nanofluid in a differential heated enclosure with non-uniform heating wall. Comprehensive review of nanofluid heat transfer in porous medium, was revealed by Nabwey *et al*. [15].

Petal et al., [16], elucidated a micro-convection model for thermal conductivity of nanofluids. Impacts of variable thermal conductivity and mixed convective stagnation-point flow in a couple stress nanofluid with viscous heating and heat source, was investigated by Gajjela and Garvandha, [17]. MHD flow and heat transfer of hybrid nanofluid over an exponentially shrinking surface with heat source/sink was lamented by Othman et al., [18]. Numerical simulation of variable thermal conductivity on 3D flow of nanofluid over a stretching sheet was explored by Tarakaramu *et al*., [19], System of equations were solved numerically by Runge-Kutta-Fehlberg scheme along with well-known shooting technique The results reviled that the temperature and velocity of the fluid rise with increasing values of variable thermal conductivity parameter. Also, the temperature and normal velocity of the fluid in case of *Cu*-water nanoparticles is more than that of Al_2O_3- water nanofluid. Abbas *et al*. [20] studied numerical analysis of MHD nanofluid flow characteristics with heat and mass transfer over a vertical cone subjected to thermal radiations and chemical reaction. Khan and Malik studied forced convective heat transfer to sisco nanofluid past a stretching cylinder in the presence of variable thermal conductivity.

The effects of slip boundary condition on the flow of fluid in a channel, was studied by Rao and Rajagopal, [21]. Mukhopadyau [22], presented slip effects of MHD boundary layer flow over an exponentially stretching sheet with suction/blowing and thermal radiation. MHD slip flow on Newtonian fluid past a stretching sheet with thermal convective boundary condition, radiation and chemical reaction, was examined by Reda and Abdel Rahman, [23]. Sher Akbar *et al.*, [24], presented radiation effect on MHD stagnation point flow of nanofluid towards stretching surface with convective boundary condition. Buoyancy effect on MHD flow of nanofluid over a stretching sheet in the presence of thermal radiation was explored by Rashid *et al.*, [25]. Hayat *et al.,* [26] demonstrated MHD three dimensional flow of nanofluid with velocity slip and non-linear thermal radiation. Daniel, [27] analysed presence of heat generation/absorption on boundary layer slip flow of nanofluid over a porous stretching sheet. Thermal radiation effects on the nanofluid buoyancy flow and heat transfer over a stretching sheet considering Brownian motion was forwarded by Doganchi and Ganji, [28]. Yashkun et al., [29] elaborated MHD hybrid nanofluid flow over a permeable stretching/shrinking sheet with thermal radiation effects. MHD flow and heat transfer of a hybrid nanofluid past a nonlinear surface stretching/shrinking with effects of thermal radiation and suction was modelled by Jaafar et al., [30]. Vishalakshi et al., [31] explored MHD hybrid nanafluid flow over a stretching/shrinking sheet with skin friction: effects of radiation and mass transpiration. Effects of slip condition and Newtonian heating on MHD flow Caisson fluid over a non-linearly stretching sheet saturated in a porous medium, was analyzed by Imran *et al.* [32]. Arabpour *et al*., [33] considered investigation into the effects of slip boundary condition on nanofluid flow in a double layer microchannel. Significance of thermal slip and convective boundary conditions in three dimension rotating Darcy-Forchheimer nanofluid flow was elucidated by Shafiq *et al*., [34] Ahmed and Sarki, [35], examined slip condition effects on unsteady MHD fluid flow with radiative heat flux over a porous medium. The result indicated that flow of fluid with higher magnetic flux can be enhanced in slip regime. Dual solution and stability analysis of Cu-H_2O-Casson nanofluid convection past a heated stretching/shrinking slippery sheet in a porous medium, was examined by Duguma et al.,[36].

Motivated by the above cited literature, the aim is to carefully study the characteristics flow pattern of hybrid nanofluid slip flow over a permeable sheet with radiative heat flux, variable thermal conductivity and heat source. This serves as extension of work of Wahid et al., [11] to include radiative heat flux and variable thermal conductivity. It may be possible to have dual solutions in the work due to nature of stretching/shrinking surface. To determine physically reliable and stable solutions the stability analysis was carried out and numerical solution of the coefficient of skin friction and rate of heat transfer are presented graphically and the results are discussed.

Mathematical Description of the Problem

A steady boundary layer of hybrid nanofluid slip flow induced by permeable stretching/shrinking sheet with radiation heat flux and heat generation is formed. We consider that the variable thermal conductivity k_{hnf} is assumed to be of the form given by Taghreed and Mahdy, [37], $k_{hnf} = k_0\left\{1+m^*\left(T-T_\infty\right)\right\}$, where k_0 and k_{hnf} are the thermal conductivities at temperatures at the wall of the sheet and ambient fluid respectively and m^* is the constant depending of the nature of the fluid. According to the physical model in figure 1, u and v are velocity in x and y directions respectively. The surface velocity is given as $u_w(x) = ce^{x/L}$ and the wall mass transfer velocity is specified as $v_w(x) = v_0 e^{x/2L}$ $\lambda \geq 0$ is the stretching constant $\lambda = 0$ refer to motionless sheet, T is the temperature, $T_w = T_\infty + T_0 e^{x/2L}$ is the sheet varying temperature with constant, T_0 and $q = q_0 e^{x/l}$ is the heat generation rate constant.

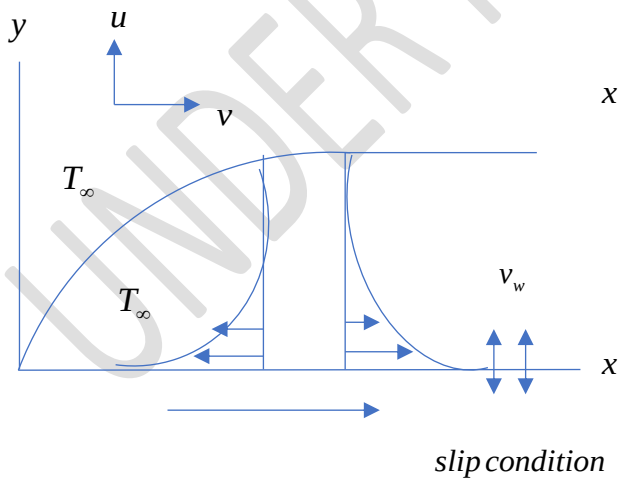

Figure 1. Physical model

Adopting the stretching/shrinking model (Wahid et al., [11]), convective transport model equations governing boundary layer for continuity, momentum and energy are given as;

$$\frac{\partial u}{\partial x}+\frac{\partial v}{\partial y}=0 \tag{1}$$

$$u\frac{\partial u}{\partial x}+v\frac{\partial v}{\partial y}=\frac{\mu_{hnf}}{\rho_{hnf}}\frac{\partial^2 u}{\partial y^2} \tag{2}$$

$$(\rho C_p)_{hnf}\left(u\frac{\partial T}{\partial x}+v\frac{\partial T}{\partial y}\right)=k_{hnf}\frac{\partial}{\partial z}\left(1+m^*(T-T_\infty)\frac{\partial T}{\partial y}\right)-\frac{\partial qr}{\partial y}-q(T-T_\infty) \tag{3}$$

The appropriate boundary conditions are as follows;

$$u=u_w(x)\lambda+P_1\frac{\mu_{hnf}}{\rho_{hnf}}\frac{\partial u}{\partial y},\quad v=v_w,\qquad T=T_w(x)+Q_1\frac{\partial T}{\partial y}\qquad at\ \ y=0 \tag{4}$$

Where P and Q are velosity and thermal slip factors respectively.

The local radiant for the case of an optically thin grey gas is expressed using Rosseland approximation and its formula derived from the diffusion concept of radiative heat transfer as

$$q_r=-\frac{4\sigma^*}{3k}\frac{\partial T^4}{\partial y} \tag{5}$$

where σ the Stefan Boltzmann constant, k the thermal conductivity of the fluid. We assume that the temperature differences within the flow are sufficiently small such that T^4 may be expressed as a linear function of the temperature. This is accomplished by expanding T^4 in Taylor series about T_∞ and neglecting higher order terms, thus

$$\left.\begin{aligned} &T^4\cong 4T_\infty^3T-3T_\infty^4\\ &q_r=-\frac{4\sigma^*}{3k_f}\frac{\partial}{\partial y}\left(4T_\infty{}^3T-3T_\infty{}^4\right)\Rightarrow\frac{\partial q_r}{\partial y}=-\frac{16\sigma^*T_\infty}{3k_f}\frac{\partial^2 T}{\partial y^2}\end{aligned}\right\} \tag{6}$$

By using equations (5) and (6), equation (2) reduces to

$$(\rho Cp)_{hnf}\left(\frac{\partial T}{\partial t}+u\frac{\partial T}{\partial x}+v\frac{\partial T}{\partial y}\right)=k_{hnf}\frac{\partial}{\partial y}\left(1+m^*(T-T_\infty)\frac{\partial T}{\partial y}\right)+\frac{16a^*\sigma T_\infty^3}{3k_f}\frac{\partial^2 y}{\partial y^2} \tag{7}$$

Hybrid Nanofluid correlations properties are represented in equation (8) to (11). These are as in (Wahid et al., [11]) and (Weni et al.[38])

$$\begin{aligned}&\rho_{hnf}=\rho_{s1}\phi_{s1}+\rho_{s2}\phi_{s2}+\rho_f\left(1-\phi_{hnf}\right)\\ &\quad where\ \phi_{hnf}=\phi_{s1}+\phi_{s2}\end{aligned} \tag{8}$$

$$(\rho C_p)_{hnf} = (\rho C_p)_{s1}\phi_{s1} + (\rho C_p)_{s2}\phi_{s2} + (\rho C_p)_f\left(1-\phi_{hnf}\right) \tag{9}$$

$$\mu_{hnf} = \mu_f\left(1-\phi_{hnf}\right)^{-2.5} \tag{10}$$

$$k_{hnf} = k_f\left(\frac{2k_f + \left(\frac{\phi_{s1}k_1+\phi_{s2}k_2}{\phi_{hnf}}\right) + 2(\phi_{s1}k_1+\phi_{s2}k_2) - 2\phi_{hnf}k_f}{2k_f - (\phi_{s1}k_1+\phi_{s2}k_2) + \left(\frac{\phi_{s1}k_1+\phi_{s2}k_2}{\phi_{hnf}}\right) + \phi_{hnf}k_f}\right) \tag{11}$$

Where ρ_s is the density of the solid nanoparticles, ρ_f is the density of the base fluid, k_s nanoparticles thermal conductivity, k_f base fluid thermal conductivity, ϕ_s nanoparticles volume fraction, and μ_f base fluid dynamic viscosity.

In order to make the fluid flow dimensionless, the following similarity quantities are introduced

$$u = \frac{\partial\psi}{\partial y}, \quad \psi = e^{x/2L}\sqrt{2\nu_f Lc}\,f(\eta,\tau), \quad \eta = ye^{x/2L}\sqrt{\frac{c}{2\nu_f L}}, \quad \nu = -\frac{\partial\psi}{\partial x} \tag{12}$$

Equation (1)-(3) transformed to non-dimensional form by using the non-dimensional variables equation (12) above to get the similarity solutions (Wahid *et al*., 2020).

$$B_1 f'''+ ff''-2f'^2 = 0 \tag{13}$$

$$B_2\left(\frac{1-\varepsilon\theta}{\Pr}\right)\theta''+B_3(f\theta'-f'\theta)+B_2\left(\frac{\varepsilon(\theta')^2}{\Pr}\right)+R\theta''+\gamma\theta = 0 \tag{14}$$

With boundary conditions as;

$$f(0) = S, \qquad f'(0) = \lambda + Pf''(0) \qquad \theta(0) = 1 + Q\theta'(0) \tag{15}$$

$$f'(\eta)\to 0, \quad \theta(\eta)\to 0, \quad as\ \eta\to\infty$$

Table 1. Thermo-physical properties of water and nano particles.

Physical properties	Water	Aluminium oxide	Silver
Density $\rho(kg/m^3)$	997.1	3970	10500
Specific heat $C_p(J/kgK)$	4179	765	235
Thermal conductivity $k(W/mK)$	0.613	40	429

Where η is the similarity variable, $\Pr$ is the Parandtl number S is the constant mass flux transfer parameter, where $S>0$ represents suction while $S<0$ represents injection of the fluid, ε which represents variable thermal conductivity parameter, R is the radiation parameter,

P is the velocity slip parameter and Q is the thermal slip parameter. The dimensionless parameters are defined as follows;

$$B_1 = \left(\frac{\mu_{hnf} / \mu_f}{\rho_{hnf} / \rho_f} \right) \qquad B_2 = \left(\frac{k_{hnf}}{k_f} \right) \qquad B_3 = \frac{(\rho C_p)_{hnf}}{(\rho C_p)_f} \quad \gamma = 2q_0 L / c(\rho C_p)_f \quad \Pr = (\mu C_p)_f / k_f$$

$$R = \frac{4\sigma T^3}{3k^*_{hnf}} \ , \varepsilon = m^*(T - T_\infty) \tag{16}$$

The wall skin friction τ_ω and heatflux q_ω are computed as

$$\tau_\omega = \mu_{nf} \left. \frac{\partial u}{\partial y} \right|_{y=0} \qquad q_\omega = k_{nf} \left. \frac{\partial T}{\partial y} \right|_{y=0} \tag{17}$$

Other physical quantities of engineering and industrial interest include the coefficient of skin friction C_f, and the local Nusselt number Nu is given by

$$C_f = \frac{\tau_\omega}{\rho_f U_\omega^2} \qquad Nu = \frac{x q_\omega}{k_f (T_f - T_\infty)} \quad \text{and} \quad \mathrm{Re}_x^{1/2} C_f = B_1 f''(0) \text{ while}$$

$$\mathrm{Re}_x^{-1/2} Nu_x = -B_2 \theta'(0) \tag{18}$$

It is possible to compute dual solutions, which enable the flow stability to be ascertained. Ignoring continuity equation, the momentum equation and energy equations are rendered time dependant by in cooperating time derivatives in equation (2) and (3);

$$\frac{\partial u}{\partial t} + u \frac{\partial u}{\partial x} + v \frac{\partial u}{\partial y} = \frac{\mu_{hnf}}{\rho_{hnf}} \frac{\partial^2 u}{\partial y^2} \tag{19}$$

$$(\rho Cp)_{hnf} \left(\frac{\partial T}{\partial t} + u \frac{\partial T}{\partial x} + v \frac{\partial T}{\partial y} \right) = k_{hnf} \frac{\partial}{\partial y} \left(1 + m^*(T - T_\infty) \frac{\partial T}{\partial y} \right) + \frac{16 a^* \sigma T_\infty^3}{3k_f} \frac{\partial^2 y}{\partial y^2} - q(T - T_\infty) \tag{20}$$

Where t denotes time.

The dimensionless quantities for time dependant variable transformation for equation (19) and (20) are

$$\eta = y e^{x/2L} \sqrt{\frac{c}{2\nu_f L}} \qquad \psi = e^{x/2L} \sqrt{2\nu_f L c} \, f(\eta, \tau) \qquad \theta(\eta, \tau) = \frac{T - T_\infty}{T_w - T_\infty} \qquad \tau = \frac{C}{2L} t e^{x/L} \tag{21}$$

Using the above quantities, equation (13) and (14) become

$$B1 \frac{\partial^3 f}{\partial \eta^3} + \frac{\partial^2 f}{\partial \eta^2} f - 2 \left(\frac{\partial f}{\partial \eta} \right)^2 - \frac{\partial^2 f}{\partial \eta \partial \tau} = 0 \tag{22}$$

$$B_2 \left(\frac{1 - \varepsilon\theta}{\Pr} \right) \frac{\partial^2 \theta}{\partial \eta^2} + B_3 \left(\frac{\partial \theta}{\partial \eta} f - \frac{\partial f}{\partial \eta} \theta - \frac{\partial \theta}{\partial \tau} \right) + B_2 \varepsilon \left(\frac{\partial \theta}{\partial \eta} \right)^2 + \frac{\partial^2 \theta}{\partial \eta^2} R + \gamma\theta = 0 \tag{23}$$

The correspondent boundary condition for the time dependent flow are;

$$f(0, \tau) = S, \ \frac{\partial f}{\partial \eta}(0, \tau) = \delta + P \frac{\partial^2 f}{\partial \eta^2}(0, \tau), \ \ \theta(0) = 1 + Q \frac{\partial \theta}{\partial \eta}(0, \tau) \tag{24}$$

$$\frac{\partial f}{\partial \eta}(\eta,\tau)\to 0,\quad \theta(\eta,\tau)\to 0 \qquad as\,\eta\to\infty$$

The perturbation equation is introduced for stability analysis of the similarity assumed solutions, $f(\eta)=f_0(\eta)$ and $\theta(\eta)=\theta_0(\eta)$

$$f(\eta,\tau)=f_0(\eta)+F(\eta)e^{-\Omega t} \tag{25}$$
$$\theta(\eta,\tau)=\theta_0(\eta)+G(\eta)e^{-\Omega t}$$

Where Ω is undetermined eigenvalue, consequently values of $F(\eta)$ and $G(\eta)$ are relatively small compared to $f_0(\eta)$ and $\theta_0(\eta)$ respectively.

Substituting equation (25) into equation (22)-(24) and also render value of τ to zero, the initial decay or growth of of disturbance in equation (25) can be traced and the linearized equations are obtained as;

$$B_1F'''+f_0''F+F''f_0-4F'f_0'+\Omega F'=0 \tag{26}$$

$$B_2\left(\frac{1-\varepsilon G}{\Pr}\right)G''+B_3(f_0G'+F\theta_0'-f_0'G-F'\theta_0-\Omega G)+2B_2\varepsilon G'\theta_0'+RG''+\Omega G=0 \tag{27}$$

And the corresponding linearized boundary conditions;

$$F(0)=0,\quad F'(0)=PF''(0),\ G(0)=QG'(0) \tag{28}$$
$$F'(\infty)\to 0 \quad \text{and} \quad G'(\infty)\to 0$$

The above linearized boundary conditions equation (28) are equated to zero. It is important to relax $F'(\infty)\to 0$ and be replaced with $F'(0)=1$ to produce realizable and stable eigenvalues.

Table 2. Validation of the present solutions of $f''(0)$ and $-\theta'(0)$ for $S=3$, $\Pr=0.7$, $\varepsilon=0$, $R=0$, and $P=Q=0$.

	$f''(0)$		$-\theta'(0)$	
	First Solution	**Second Solution**	**First Solution**	**Second Solution**
Hafidzuddin et al., [39]	2.3908	-0.9722	1.7712	0.8432
Waini *et al.,* [38]	2.390814	-0.972247	1.771237	0.848316
Wahid *et al.,* [11]	2.390813	-0.972129	1.771237	0.847748
Present Result	2.390813634	-0.97212884	1.771237309	0.847748178

Result and Discussion

The result of the combined effects of the solution of the equation (13) and (14) under condition in equation (15) are obtained using bvp4c solver in MATLAB software. The single phase nanofluid flow model under investigation is a hybrid nanoparticles aluminium oxide and silver with water base fluid , the effective parandtl number of working nanofluid is that of pure water (i.e Pr = 0.62) (Yashkun et al., 2020).

The stretching as indicated in equation (15) is where $(\lambda > 0)$ while shrinking is $(\lambda < 0)$. Radiative heat flux, variable thermal conductivity, velocity slip parameter, thermal slip parameter, and nano volume fraction for silver are varied in order to study their impacts on the flow. Prantln number and aluminium nano volume fraction are specified fixed throughout the study as $\Pr = 0.62$ and $\phi_1 = 0.01$.

The temperature profile $\theta(\eta)$ for varied values of variable thermal conductivity parameter (ε) is indicated in figure 2. The result indicated that upsurge in variable thermal conductivity parameter generates increase in temperature for second solution, but decrease in first solution. It indicates that in a shrinking region heat absorption take place with increase in value of variable thermal conductivity parameter. Figure 3 indicates the influence of radiative flux on temperature profile $\theta(\eta)$, as expected it is noticed that increase in radiative parameter attracts increase in temperature of the fluid. This shows that presence of nano volume fraction in the fluid does not affect the influence of radiation on increasing fluid temperature at the shrinking region.

Figure 4 and 5 depict the velocity profiles $f'(\eta)$ for silver volume fraction $\phi_2 = (0.01, 0.005, 0.001)$ and velocity slip parameter P = (0.2, 0.4, 0.6). It is noticed in figure 4 reveals that as the volume fraction of nano particle decreases, the first solution indicates that velocity upsurge, in the second solution the velocity decrease. Physically it means that decrease in the size of nano particle result in decrease in the flow resistance thereby allowing more fluid flow. In figure 5, portrays the increment in P parameter which attributes to more fluid flow in the first solution and resistance to the flow in the second solution. Slip parameter stimulates boundary layer of the plate and allow more fluid to flow, that what it is in the first solution and second solution demonstrates opposite trend.

The effects of skin friction coefficient $\mathrm{Re}_x^{1/2} C_f$ on velocity slip parameter P is plotted against shrinking/stretching parameter λ as depicted in figure 6. Bifurcation of boundary layer shift slightly with increase in P at a certain point in shrinking region where (λ= -2.0783), (λ = -1.7652) and (λ = -1.4662) in the first solution and the trend changes gradually toward stretching region (λ > 0).

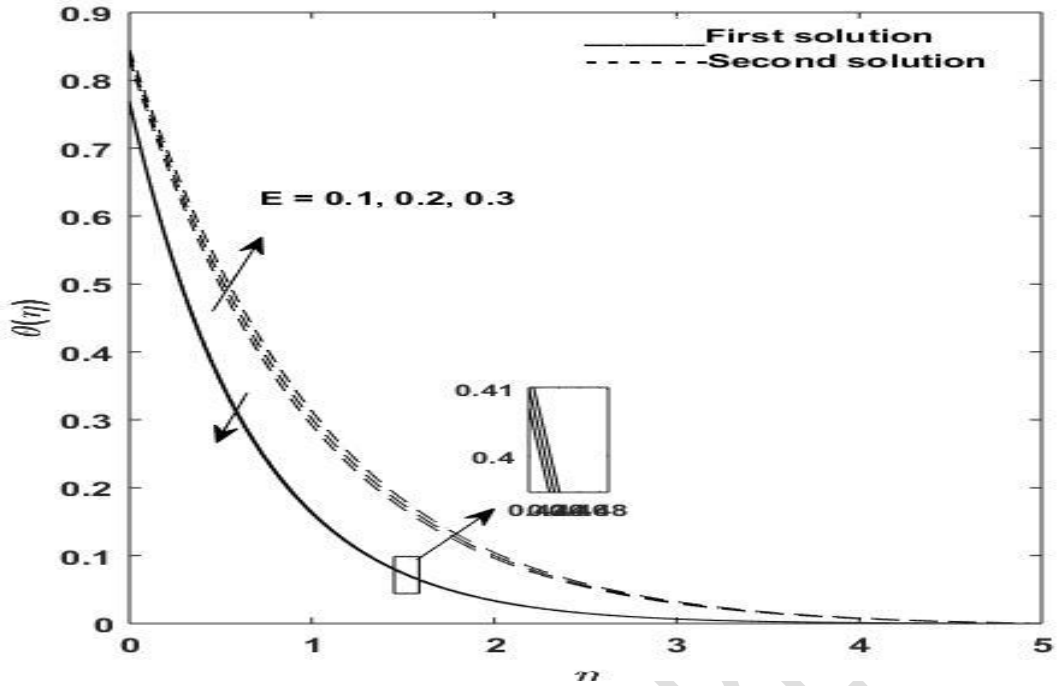

Figure 2. Dual solution for temperature profile variable thermal conductivity parameter (Ɛ)

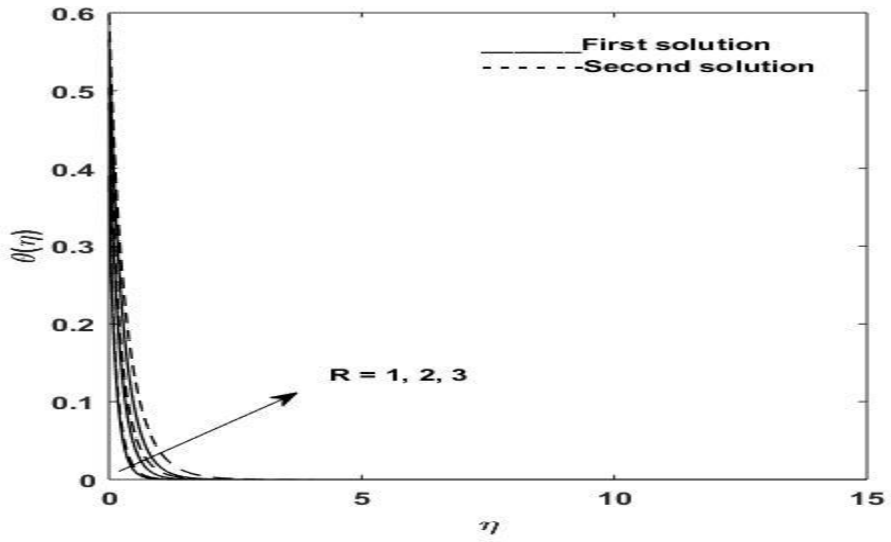

Figure 3. Dual solution of temperature profile for radiative heat flux (R)

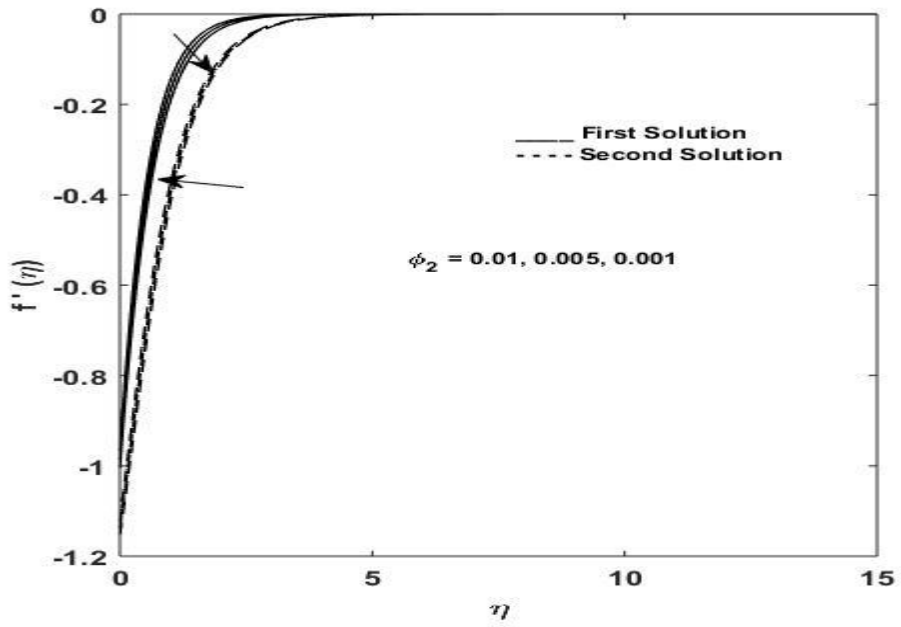

Figure 4. Dual solution of velocity profile ϕ_2

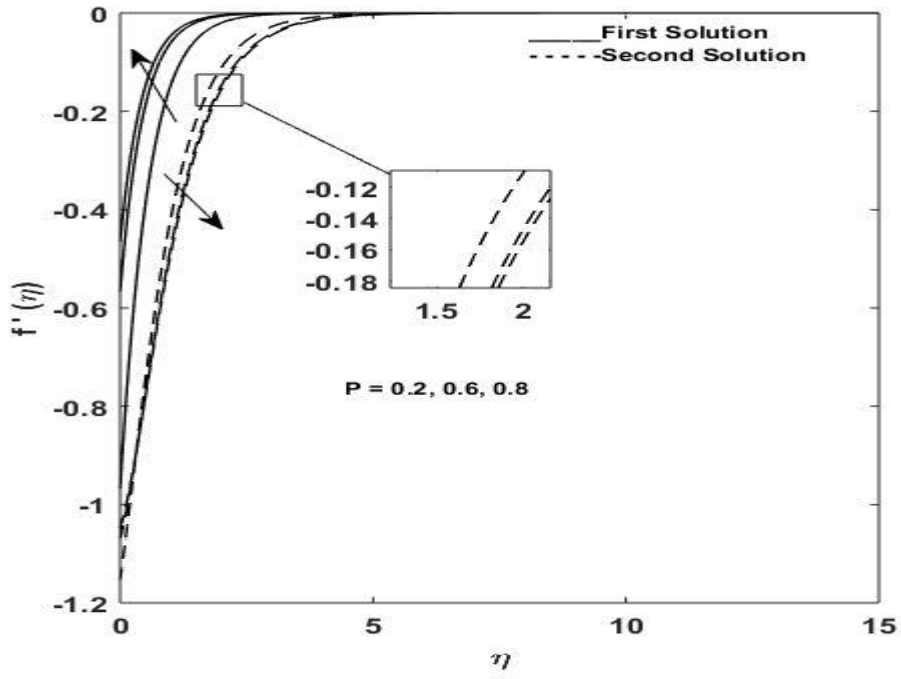

Figure 5. Dual solution of velocity slip parameter (P)

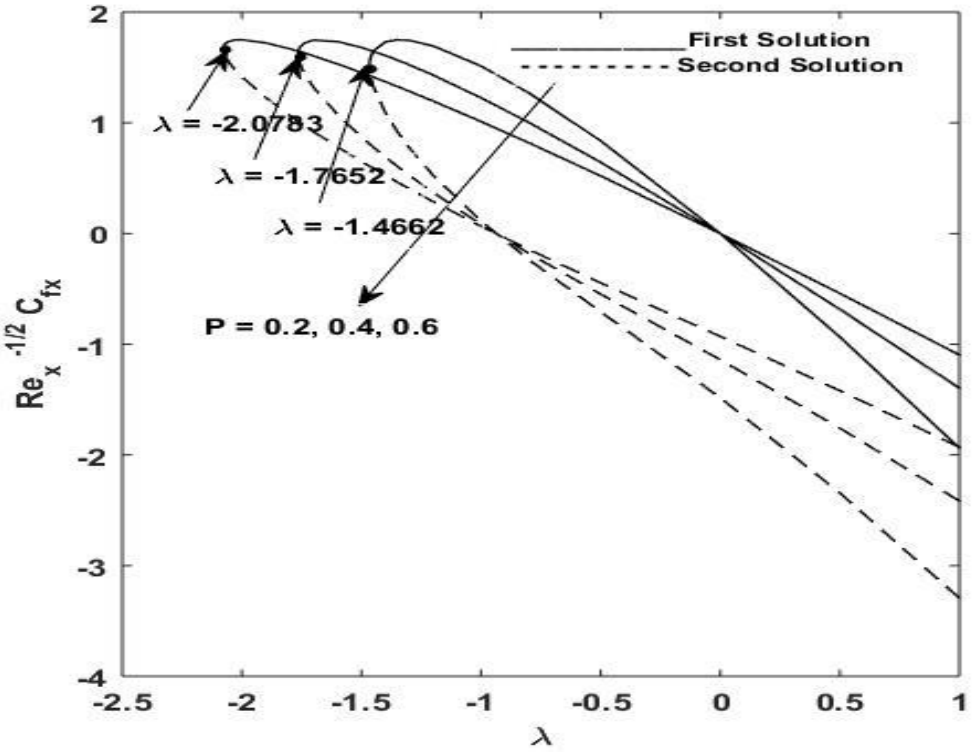

Figure 6. Local Skin friction on λ for varied values of P

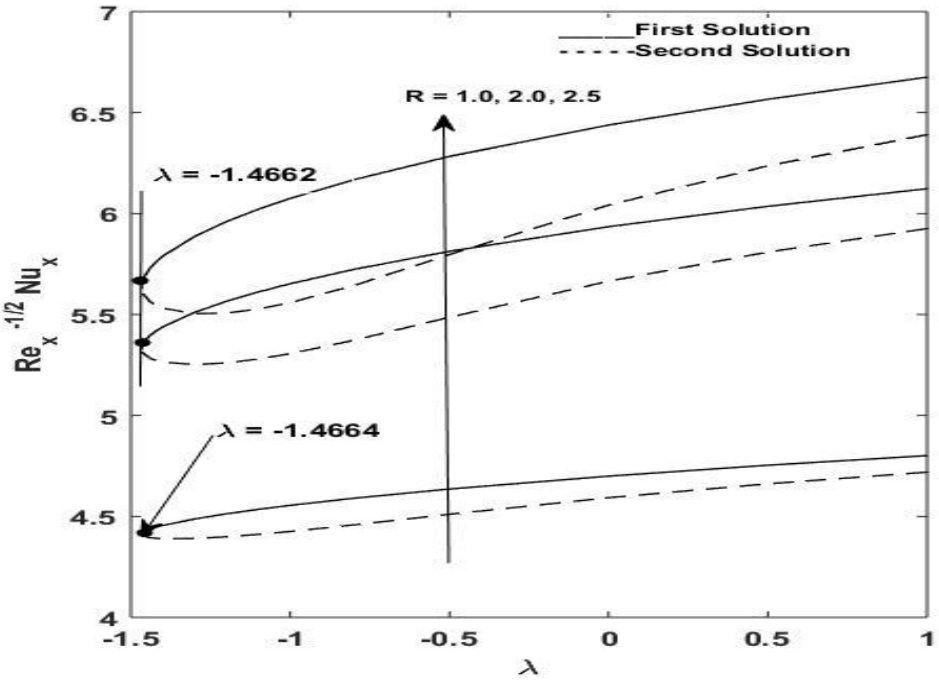

Figure 7. Local Nusselt's number on λ with varied R

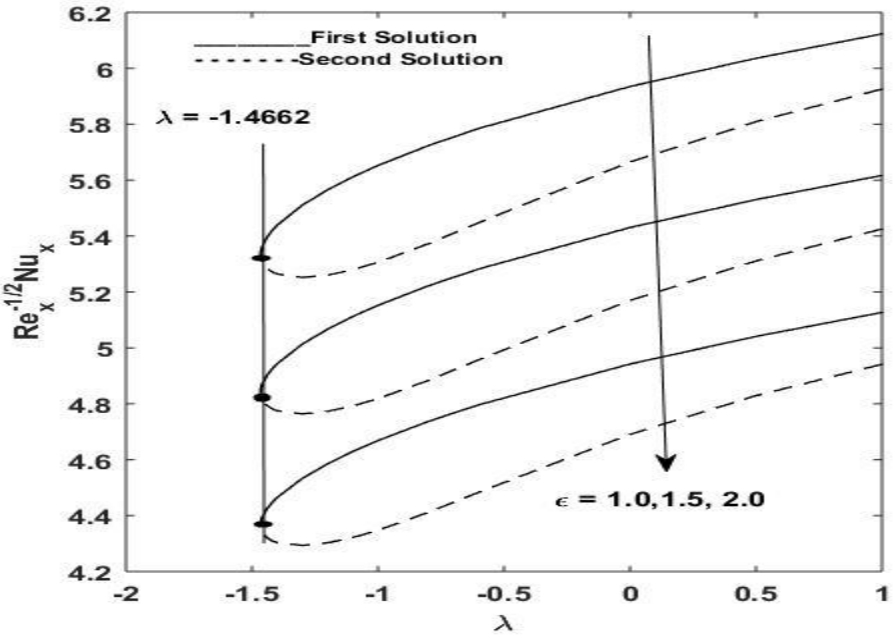

Figure8. Local Nusselt's number on λ for varied values of ε

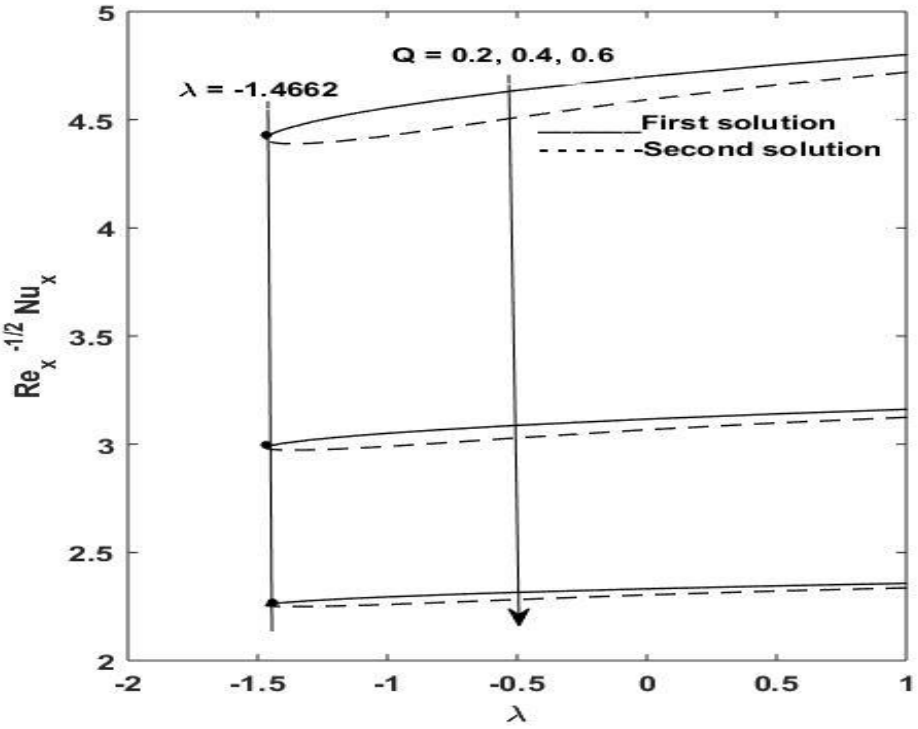

Figure 9. Loval Nusselt's number on λ for varied values of Q

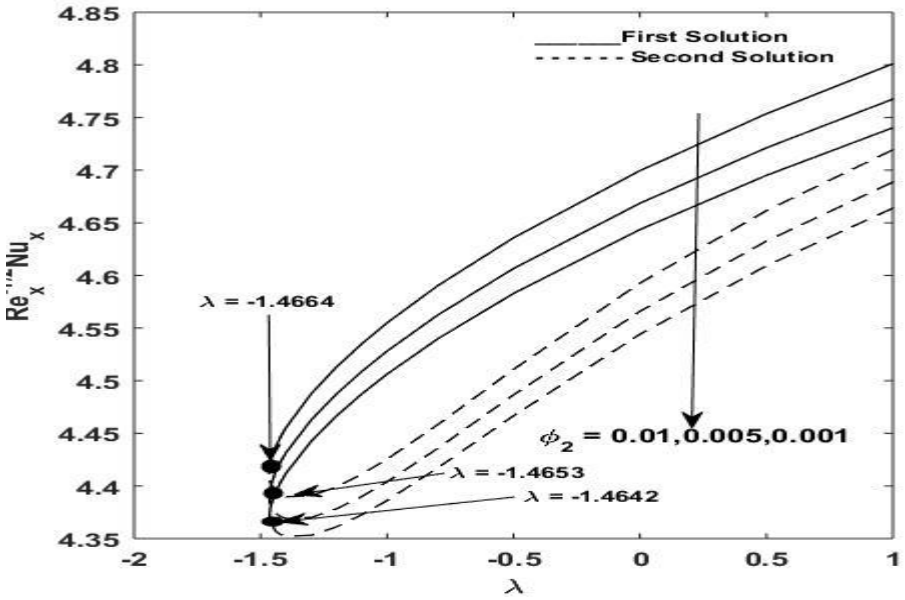

Figure 10. Local Nusselt's number on λ for varied values of ϕ_2

The upsurge in radiation parameter R leads to increase in rate of heat transfer $\mathrm{Re}_x^{-1/2} Nu_x$. Bifurcation point remain constant (λ = -1.4662) when R = 1.0, 2.0, 2.5, this is demonstrated in figure 7. Physically it means that the heat generated by R caused the local Nusselt number $\mathrm{Re}_x^{-1/2} Nu_x$ increased and bifurcation remains in shrinking region (λ< 0).

Figure 8 and 9, the impact of different values of the involving parameters on the local Nusselt number $\mathrm{Re}_x^{-1/2} Nu_x$ for shrinking/stretching parameter λ are presented. It is noticed in figure 8 that increase in variable thermal conductivity parameter reduces the local Nusselt number in both first and second solution. Concurrently the local Nusselt number is also noted to drastically reduce as value of thermal slip parameter (Q) increases. The critical point for both the plots remain in shrinking region. Physically it means that rate of heat transfer can be reduced by increasing thermal slip parameter.

For silver volume fraction ϕ_2 = (0.01, 0.005, 0.001) as reported in figure 10, the increase in silver volume fraction parameter amplifies the local Nusselt number $\mathrm{Re}_x^{-1/2} Nu_x$. Physically it shows that the rate of heat transfer in the fluid is raised with upsurge in size of silver nano particles.

Conclusion.

Hybrid nanofluid slip flow over a permeable sheet with radiative heat flux, variable thermal conductivity and heat source. The governing equations in partial differential equations of momentum and energy were converted into non dimensional ordinary differential equations using similarity transformations and solve numerically using MATLAB bvp4c solver. The conclusion is arrived with after analysis of the results as follows;

i) It indicates that on shrinking region heat absorption take place with increase in value of variable thermal conductivity parameter (Ɛ).

ii) It is noticed that increase in radiative parameter attracts increase in temperature of the fluid at the shrinking region.

iii) The velocity of the fluid is appreciated with increase in silver volume fraction (ϕ_2) and depreciates with increase in velocity slip parameter (P)

iv) Increase in velocity slip parameter decreases the local skin friction (P) and local Nusselt number is appreciated by increasing radiation parameter (R).

v) Heat absorption is noticed with increase in variable thermal conductivity, silver volume fraction (ϕ_2) and heat source/sink parameter (Q).

Reference

[1] Wen, D. & Ding, Y. (2004). Experimental investigation into convective heat transfer of a nanofluid at the entrance region under laminar flow conditions. *International Journal of Heat and Mass Transfer*. 47, 5181-5188.

[2] Roy, G., Palm, S. J. & Nguyen, C. T. (2004). Heat transfer and fluid flow of a nanofluid in laminar radial flow cooling system. *Journal of Thermal Science.* 14(4), 362-367l,

[3] Devi, A. S. P., & Andrews, J. (2011). Laminar boundary layer flow of nanofluid over a flat plate. *International Journal of Applied Mathematics and Mechanics.* 7(6), 52-71.

[4] Hamad, M. A. A. (2011). Analytical solution of natural convection flow of a nanofluid over a linearly stretching sheet in the presence of magnetic field. International Communication in Heat and Mass Transfer, 38(4), 487-492. Dx.doi.org/10.1016/j.icheatmasstransfer.2010.12.042.

[5] Maripola, S., & Kishan, N. (2017). MHD nanofluid radiating stretching sheet with chemical reaction and heat source/sink. *International Journal of Innovation Research in Science, Engineering and Technology*. 6(2), 15999-16007.

[6] Aly, E. H. & Pop, I. (2019). MHD flow and heat transfer over a permeable Stretching /shrinking sheet in a hybrid nanofluid with a convective boundary condition. *HFF 2019*, 3012-3038.

[7] Lund, L. A., Omar Z., Khan I. and Sherif E. S. M. (2020). Dual solutions and stability analysis of a hybrid nanofluid over a stretching/shrinking sheet executing MHD flow. Symmetry. 12, 276.

[8] Zainal A. N., Nazar, R., Nayanthrun K. and Pop I. (2020). Stability analysis of MHD hybrid nanofluid flow over a stretching/shrinking sheet with quadratic velocity. *Alexzandria Engineering Journal*. https://doi.org/10.1016/j.aej.2020.10.020

[9] Xuan, Y. & Roetzel, W. (2000). Conceptions for heat transfer correlation of nanofluids. *International Journal of Heat and Mass Transfer*. 43, 3701-3707.

[10] Huang, C. J., & Yih, K. U. (2021). Non-Linear radiation and variable viscosity effects on free convection of a .power-law nanofluid over a truncated cone in a porous media with zero nanoparticles flux and internal heat generation. *Journal of Thermal Science and Engineering Applications*. Vol. 13/031020-1

[11] Wahid, N. S., Arifin, N. M., Khashi'ie N. S., and Pop I. (2021). Hybrid nanofkuid slip flow over an exponentially stretching/shrinking permeable sheet with heat generation. *Mathematics*. 9, 30.dx.doi.org/1o.3390/math90 10030.

[12] Gangadha, K., Kakshmi, B. K., El-Sapa, S., Subbarae, M. V. & Chamkha, A. J. (2022). Thermal energy transport of radioactive nanofluid flow submerged with microorganisms with zero mass flux condition. *Waves in Random and Complex Media*. https:/doi.org/10.1080/17455030.2022.2072536.

[13] Iyahraja S., Rajadurai S. J., Sivakumar, M. and Lenin N. (2022). Investigation on silver-water nanofluid for development of new viscosity correlation. *Bull. Chem. Ethiop*. 37(2), 505-514

[14] Rajesh, V. & Sheremet, M. (2023). Natural convection of ternary nanofluid in a differential heated enclosure with non-uniform heating wall. *Micromachnics*. 14, 1049 https://doi.org/10.3390/mi14051049.

[15] Nabwey, H., A., Armaghani, T., Azizimehr, B., Rashad, A. M. & Chamkha, A., J. (2023). Comprehensive review of nanofluid heat transfer in porous medium. *Nanomaterials.* 13, 937 https://doi.org/10.3390/nano13050937.

[16] Patel H. E., Sundararajan T., Paradeep T., Dasgupta A., Dasgupta N. and Das S. K. (2005). A micro-convection model for thermal conductivity for nanofluids. Paramana Journal of Physics, 65(5), 863-869. Doi.org/10.1007/bf02704086

[17] Gajjela N. and Garvandha M. (2020). Impacts of variable thermal conductivity and mixed convective stagnation point flow in a couple stress nanifluid with viscous heating and heat source. Heat Transfer. 49(6), 3630-3650.https://doi.org/10.1002/htj.21792.

[18] Othman, M. N., Jedi, A. Bukar N. A. A. (2021). MHD flow and heat transfer of hybrid nanofluid over an exponentially shrinking surface with heat source/sink. Appl. Sci. 11, 8199. Doi.org/10.3390/app11178199.

[19] Tarakaramu, N., Narayana P. V. S. and Venkateswarlu B. (2020). Numerical simulation of variable thermal conductivity on 3D flow of nanofluid over a stretching sheet. *Nonlinear Engineering*, 9(1), 233-243.

[20] Abbas, W., Ibrahim A.M., Mokhtar O., Megahed A. M. and Said A. A. M. (2023). Numerical analysis of MHD nanofluid flow characteristics with heat and mass transfer over a vertical cone subjected to thermal radiations and chemical reaction. *Journal of Nonlinear Mathematical Physics*. Doi.org/10.1007/s44198-023-00142-4

[21] Rao I. J. and Rajagopal K. R. (1999). The effects of the slip boundary condition on the flow of fluid in a channel. *Acta Mechanics*. 135, 113- 126.

[22] Mukhopadhyau S. (2013). Slip effects on MHD boundary layer flow over an exponentially stretching sheet with suction/blowing and thermal radiation. *Ain Shams Engineering Journal*. 4(3), 485-491

[23] Reda, G. & Abdel R. (2013). MHD slip flow on Newtonian fluid past a stretching sheet with thermal convection boundary condition, radiation and chemical reaction. *Hindawi Publishing Cooperation, Mathematical Problems in Engineering*. Article ID 359817, 1-12.

[24] Sher-Akbar M., Nadeem S., Ul-Haq R. and Khan Z. H. (2013). Radiation effects on MHD stagnation point flow of nanofluid towards stretching surface with convective boundary condition. *Chinese Journal of Aeronautics*. 26(6), 1389-1397.

[25] Rashid M. W., Ganesh N. V., Abdul-Hakim A. K and Gangi B. (2014). Buoyancy effects on MHD flow of nanofluid over a stretching sheet in the presence of thermal radiation. *Journal of Molecular Liquids*. 198, 234-238.

[26] Hayat T., Imtiaz M., Alsaed A. and Kutbi M. A. (2015). MHD three dimensional flow of nanofluid with velocity slip and non-linear thermal radiation. *Journal of Magnetism and Magnetic Materials*. 396, 31-37.

[27] Daniel Y. (2015). Presence of heat generation/absorption on boundary layer slip flow of nanoafluuid over a porous stretching sheet. American Journal of Heat and mass transfer. 2(1), 15-30. Hppts;//dx.doi.org/10.7726/ajhmt.2015.100

[28] Doganchi A. and Ganji D. D. (2016). Thermal radiation effects on the nanofluid buoyancy flow and heat transfer over a stretching sheet considering Brownian motion. *Journal di Molecular Liquids*. 223, 521- 527.

[29] Yashkun U., Nor H. Z., Abubakar A., Shok A. and Pop I. (2020). MHD hybrid nanofluid flow over a permeable stretching/shrinking sheet with thermal radiation effects. International Journal for Numerical methods for Heat and Fluid Flow. 0961-5539 DOI10.1108/HFF-02-2020-0083

[30] Jaafar, A. Waini, I. Jamaludin A. Nazar, R. and Pop I. (2022). MHD flow and heat transfer of a hybrid nanofluid past a nonlinear surface stretching/shrinking with effects of thermal radiation and suction. *Chinese Journal of Physics*. 79(2022), 13-27.

[31] Vishalakshi, A. B., Mahesh, R., Mahabaleshwar, U. S., Rao, A. K., Perez L. M. and Lorez D. (2023). MHD hybrid nanofluid flow over a stretching/shrinking sheet with skin friction: Effects of radiation and mass transpiration. *Magnetochemistry.* 9, 118. Doi.org/10.3390/magnetochemistry9050118

[32] Imran, U., Sharidan, S. & Ilyas K. (2016). Effects of slip condition and Newtonian heating on MHD fluid over a non-linearly stretching sheet saturated in a porous medium. *Journal of King of Saudi University Science*. 29(2), 1-10.

[33] Arabpour A., Karimipour A., Tagraic D. and Akabari O. A. (2018). Investigation into the effects of slip boundary condition on nanofluid flow in a double layer microchannel. Journal of Thermal Anal Colarim. 131, 2975-2991. Doi.org/10.1007/s10973-01-6813-3

[34] Shafiq, G. R. and Khalique C. M. (2020). Significance of thermal slip and convective boundary conditions in three dimension rotating Darcy-Forchheimer nanofluid flow. Symmetry. 12(5), 741. Doi.org/10.3390/sym12050741.

[35] Ahmed A. and Sarki M. N. (2023). Slip condition effects on unsteady MHD fluid flow with radiative heat flux over a porous medium. *Advances in Pure Mathematics*, 13, 153-166. https://doi.org/10.4236/apm.2023.133008.

[36] Duguma K. A., Makinde O. D. and Eyadene G. L. (2023). Dual solution and stability analysis of Cu-H_2O-Casson nanofluid convection past a heated stretching/shrinking slippery sheet in a porous medium. Hindawi Computational and Mathematical Method, ID 6671523, 20. Hppts://doi.org/10.1155/2023/6671523.

[37] Taghreed A. H. and Mahdy A. (2022). Variable thermal conductivity and thermophoric aspects of free convection flow of a macropolar fluid due to permeable cone: heat source/sink. *AIP Advances.* 12, 095308.

[38] Waini, I., Ishak, A. and Pop, I. (2019). Hybrid nanofluid flow induced by an exponentially shrinking sheet. *Chinese Journal of Physics.*

[39] Hafidzuddin, M. E. H., Nazar R., Arifin N. M. and Pop I. (2016). Boundary layer flow and heat transfer over a permeable exponentially stretching/shrinking sheet with generalized slip velocity. *JAFM*, 9, 2025-2036